REGULAR ARTICLE

blood advances

The hematopoietic stem cell marker VNN2 is associated with chemoresistance in pediatric B-cell precursor ALL

Beat Bornhauser,[1,*] Gunnar Cario,[2,*] Anna Rinaldi,[1,*] Thomas Risch,[3,*] Virginia Rodriguez Martinez,[1,*] Moritz Schütte,[4,*] Hans-Jörg Warnatz,[3] Nastassja Scheidegger,[1] Paulina Mirkowska,[1] Martina Temperli,[1] Claudia Möller,[1] Angela Schumich,[5] Michael Dworzak,[5] Andishe Attarbaschi,[5] Monika Brüggemann,[6] Mathias Ritgen,[6] Ester Mejstrikova,[7] Andreas Hofmann,[8] Barbara Buldini,[9] Pamela Scarparo,[9] Giuseppe Basso,[9,10] Oscar Maglia,[11] Giuseppe Gaipa,[11] Tessa Lara Skroblyn,[12] Quy A. Ngo,[1] Geertruij te Kronnie,[9] Elena Vendramini,[9] Renate Panzer-Grümayer,[5] Malwine Jeanette Barz,[1] Blerim Marovca,[1] Mathias Hauri-Hohl,[13] Felix Niggli,[1] Cornelia Eckert,[12] Martin Schrappe,[2] Martin Stanulla,[14] Martin Zimmermann,[14] Bernd Wollscheid,[8] Marie-Laure Yaspo,[3] and Jean-Pierre Bourquin,[1]

[1]Department of Oncology, University Children's Hospital Zurich and Children's Research Center, Zurich, Switzerland; [2]Department of Pediatrics, University Medical Center Schleswig-Holstein, Campus Kiel, Kiel, Germany; [3]Department of Vertebrate Genomics, Max Planck Institute for Molecular Genetics, Berlin, Germany; [4]Alacris Theranostics, Berlin, Germany; [5]St. Anna Children's Hospital and Children's Cancer Research Institute, Vienna, Austria; [6]Department of Hematology, University Hospital Schleswig-Holstein, Kiel, Germany; [7]Department of Pediatric Hematology and Oncology, Charles University Hospital Motol, Prague, Czech Republic; [8]Department of Health Sciences and Technology and Institute for Molecular Systems Biology, ETH Zurich, Zurich, Switzerland; [9]Department of Women's and Children's Health, University of Padova, Padova, Italy; [10]Italian Institute for Genomic Medicine, Turin, Italy; [11]M. Tettamanti Research Center, University of Milano Bicocca, Monza, Italy; [12]Pediatric Hematology and Oncology, Charité University Hospital, Berlin, Germany; [13]Department of Stem Cell Transplantation, University Children's Hospital Zurich, Zurich, Switzerland; and [14]Pediatric Hematology and Oncology, Hannover Medical School, Hannover, Germany

Key Points

- Expression of VNN2 identifies B-cell precursor ALL cases with increased resistance to chemotherapy.
- VNN2 positivity occurs across different genomic ALL subtypes and is associated with mutations in epigenetic regulators.

Most relapses of acute lymphoblastic leukemia (ALL) occur in patients with a medium risk (MR) for relapse on the Associazione Italiana di Ematologia e Oncologia Pediatrica and Berlin-Frankfurt-Münster (AIEOP-BFM) ALL protocol, based on persistence of minimal residual disease (MRD). New insights into biological features that are associated with MRD are needed. Here, we identify the glycosylphosphatidylinositol-anchored cell surface protein vanin-2 (VNN2; GPI-80) by charting the cell surface proteome of MRD very high-risk (HR) B-cell precursor (BCP) ALL using a chemoproteomics strategy. The correlation between VNN2 transcript and surface protein expression enabled a retrospective analysis (ALL-BFM 2000; N = 770 cases) using quantitative polymerase chain reaction to confirm the association of VNN2 with MRD and independent prediction of worse outcome. Using flow cytometry, we detected VNN2 expression in 2 waves, in human adult bone marrow stem and progenitor cells and in the mature myeloid compartment, in line with proposed roles for fetal hematopoietic stem cells and inflammation. Prospective validation by flow cytometry in the ongoing clinical trial (AIEOP-BFM 2009) identified 10% (103/1069) of VNN2$^+$ BCP ALL patients at first diagnosis, primarily in the MRD MR (48/103, 47%) and HR (37/103, 36%) groups, across various cytogenetic subtypes. We also detected frequent mutations in epigenetic regulators in VNN2$^+$ ALLs, including histone H3 methyltransferases *MLL2*, *SETD2*, and *EZH2* and demethylase *KDM6A*. Inactivation of the *VNN2* gene did not impair leukemia repopulation capacity in xenografts. Taken together, VNN2 marks a cellular state of increased resistance to chemotherapy that warrants further investigations. Therefore, this marker should be included in diagnostic flow cytometry panels.

Submitted 6 September 2019; accepted 29 May 2020; published online 27 August 2020. DOI 10.1182/bloodadvances.2019000938.

*B. Bornhauser, G.C., A.R., T.R., V.R.M., and M. Schütte contributed equally to this work.

For original data, please contact Jean-Pierre Bourquin (jean-pierre.bourquin@kispi.uzh.ch).

The full-text version of this article contains a data supplement.

Introduction

Despite the remarkable improvements in molecular classification,[1] our understanding of the factors associated with treatment resistance remains scarce. Thus far, assessment of minimal residual disease (MRD) remains 1 of the most important parameters for risk stratification in acute lymphoblastic leukemia (ALL).[2] More recently, improved classifiers were proposed based on the combination of cytogenetic information and MRD. Such a score can help to classify patients with a very low risk for relapse,[3,4] providing a rationale to decrease treatment intensity. Markers to identify patients at very high risk (VHR) for relapse have been defined for rare subgroups, such as *TCF3-HLF*$^{+}$ ALL,[5] hypodiploid ALL,[6] or *KMT2A* (*MLL*) rearrangements.[7] On the Associazione Italiana di Ematologia e Oncologia Pediatrica and Berlin-Frankfurt-Münster (AIEOP-BFM) ALL 2009 treatment protocol,[2] the majority of relapses occur in the group of patients who are at medium risk (MR) by MRD. Recently, a subgroup with very poor outcome has been identified with deletions in *IKAROS*, together with other mutations (IKZF1^{plus}).[8] The significance of *BCR-ABL*–like mutations in tyrosine kinase genes[9] for VHR for relapse classification remains to be clarified, because precise information from next-generation sequencing is emerging.[1] Clearly, more efforts are needed to improve our understanding and molecular classification of resistant disease.

Mapping the leukemic cell surface more precisely will be relevant in the era of antigen receptor–directed immunotherapy. Using the chemoproteomics cell surface capturing (CSC) technology to phenotype cells without antibodies, a bird's eye view of the repertoire of expressed cell surface proteins and their relative abundance ("surfaceome") can be determined in development[10] and disease.[11,12] Here, we report about surfaceome proteins that are differentially present on leukemia cells with increased resistance to conventional treatment in ALL compared with good-risk ALL and identify an association between the glycosylphosphatidylinositol (GPI)-anchored surface protein vanin-2 (VNN2; GPI-80) and MRD in the AIEOP-BFM ALL 2009 study. The human vanin gene family consists of *VNN1*, *VNN2*, and *VNN3*, whereas in mice, only *Vnn1* and *Vnn3* orthologs have been identified.[13] Human VNN1 and VNN2 are membrane-associated proteins, whereas VNN3 lacks GPI anchoring and is secreted.[14] The function of the vanin family remains to be explored. VNN1 has pantetheinase activity to generate pantothenic acid and cysteamine, activating stress pathways and inflammation by inhibition of gluthatione.[14,15] Additionally, VNN1 is involved in the thymus homing of immature T lymphocytes in mice.[16] VNN2 is mainly expressed in the hematopoietic system on myeloid cells and, to a lesser extent, on lymphoid cells, contributing to leukocyte adhesion and migration to inflammatory sites.[17] Recently, VNN2 has been implicated as a human fetal liver hematopoietic stem cell (FLHSC) marker, identifying a subset of FLHSCs in xenotransplantation assays,[18] as well as a marker of CD34^{-} human cord blood–derived primitive hematopoietic stem cells (HSCs).[19] Our study establishes the association between VNN2 and drug resistance across different molecular leukemia subtypes, providing a new marker for phenotypic exploration.

Materials and methods

Patient material

Patient specimens were included for the retrospective analysis of patients who were enrolled on the ALL-FM 2000 trial (NCT00430118) between June 1999 and December 2004, according to availability in the central biological specimen bank (supplemental Figure 1A). The characteristics of this cohort are provided in Table 1.[20] The prospective analysis was performed by the reference laboratories of the AIEOP-BFM ALL 2009 (NCT01117441) for patients enrolled between 2009 and 2018. Relapse samples were available from patients included in the BFM relapse trial 2002 (ALL-REZ BFM 2002; NCT00114348). Informed consent, in accordance with the Declaration of Helsinki, was obtained for all patients. Patients were classified as standard risk (SR), MR, or high risk (HR) for relapse, according to the clinical criteria used in the ALL-BFM 2000 trial.[21,22] Briefly, HR patients are those presenting with 1 of the following features: poor response to prednisone, no complete remission at the end of induction on day 33, MRD $\geq 1 \times 10^{-3}$ after consolidation at time point 2 (day 78), or *KMT2A-AFF1* positivity. SR patients are MRD negative at the end of induction (day 33) and after consolidation (day 78), with ≥ 2 markers with a sensitivity of 10^{-4} and no HR criteria. All other patients were classified as MR.

Identification of proteins that are preferentially expressed in HR ALL

To select proteins preferentially identified in HR ALL, we used a proteomics dataset that was obtained using CSC technology, as previously reported.[12] To identify the ALL surfaceome proteotype, cell surface residing glycoproteins were chemically tagged on living cells and subsequently analyzed by data-dependent acquisition mass spectrometry.[12] A comparable number of peptides that were matched to proteins were identified in VHR and SR patients, with an average 5481 peptides in SR ALL and 5714 peptides in VHR ALL. Data from Mirkowska et al[12] are included in supplemental Table 1. To identify candidates of the cell surface proteome that are expressed more often at the surface of 8 HR ALL samples compared with the 11 SR ALL samples in that dataset, we filtered for proteins that are identified in $\geq$50% of all HR cases ($\geq$4/8 samples) and not more than 30% of SR cases ($\leq$3 samples).

Immunophenotyping

Immunophenotyping was done in the corresponding BFM centers, and data were generated using the stringent diagnostic standards developed and approved by the AIEOP-BFM ALL FLOW-SG,[23] which are based on 2016 World Health Organization criteria, the EGIL classification, and the Bethesda 2006 recommendations.

Validation of VNN2 antibodies by flow cytometry and definition of VNN2 positivity

We tested 2 commercial monoclonal VNN2 antibodies: 1 that was generated with recombinant human VNN2 (clone 04) and another that was generated with extracts from neutrophils (clone 3H9). We stained 3 human leukemia samples and observed a stronger signal with the 3H9 clone (supplemental Figure 1B). We further validated this clone by staining peripheral blood (PB) cells from a healthy adult donor (supplemental Figure 1C) and by generating lentiviral VNN2-knockout patient-derived xenograft (PDX) cells and VNN2-overexpressing cells (supplemental Figure 1D).

To define positivity in patient samples, the internal cross-lineage CD45^{bright} lymphocyte population for each sample was used to set the VNN2 gate. The frequency of VNN2 positivity was evaluated

Table 1. Clinical features of VNN2$^+$ patients

Classifier	Retrospective cohort (PCR)	Retrospective cohort (PCR)	Prospective cohort (FACS)	Retrospective cohort (n = 770)	ALL-BFM-2000 (n = 4152)
VNN2	Negative	Positive	Positive		
	615 (79.8)	155 (20.1)	72 (—)		
Age at diagnosis, y					
1-10	456 (74.1)	101 (65.1)	41 (57.9)	557 (72.3)	3099 (74.6)
≥10	159 (25.8)	54 (34.8)	31 (43.0)	213 (27.6)	1053 (25.4)
WBC count, $\times 10^9$/L					
<50	458 (74.4)	89 (57.4)	52 (72.2)	547 (71.0)	3351 (80.7)
50-100	74 (12.0)	28 (16.1)	5 (6.9)	102 (13.2)	383 (9.2)
≥100	83 (13.4)	38 (24.5)	3 (4.1)	121 (15.7)	403 (9.7)
CNS status					
Negative (1)	518 (84.2)	134 (86.4)	53 (73.6)	712 (92.5)	3757 (90.7)
Positive (2, 3)	22 (3.5)	10 (6.4)	12 (16.6)	32 (4.1)	142 (3.4)
Risk (MRD)					
SR	209 (33.9)	32 (20.6)	18 (25.0)	241 (31.2)	1341 (32.3)
MR	268 (43.5)	78 (50.3)	4 (66.6)	346 (44.9)	1779 (42.8)
HR	30 (4.9)	14 (9.0)	37 (51.4)	44 (5.7)	146 (5.9)
TEL-AML1					
Negative	434 (70.6)	135 (87.7)	69 (95.8)	569 (73.8)	3019 (74)
Positive	160 (26.0)	16 (10.3)	3 (4.1)	176 (22.8)	868 (20.9)
KMT2A					
Negative	612 (99.5)	152 (99.5)	71 (99)	764 (99.2)	4130 (99.5)
Positive	3 (0.2)	3 (0.2)	1 (1.3)	3 (0.5)	6 (0.8)
CRLF2 aberrations					
Immunoglobulin H fusion	4 (0.6)	— (—)	1 (1.3)	4 (0.7)	4 (0.5)
P2RY8 fusion	16 (2.6)	3.2 (—)	— (—)	21 (2.7)	21 (2.7)
3X CRLF2	20 (3.2)	4 (2.5)	— (—)	24 (3.1)	24 (3.1)

All data are n (%).
—, no sample of the corresponding genetic group observed; WBC, white blood cell.

based on the standard operating procedure of AIEOP-BFM ALL Immunophenotyping Consensus Guidelines.[23] A frequency of VNN2$^+$ cells ≥10% of control was considered positive for VNN2. To define positivity in xenograft samples, we used a fluorescence-minus-one control, which consisted of a sample stained with all antibodies except VNN2. VNN2 staining always detected a homogeneous population with increased fluorescence compared with in-sample control lymphocyte populations.

Quantitative polymerase chain reaction

Total RNA was isolated with TRIzol reagent and subsequently extracted with an RNeasy Mini Kit (cat. no, 74106; Qiagen), according to standardized protocols. The amount and quality of the extracted RNA were measured with a spectrophotometer (Nanodrop ND-1000) and a Bioanalyzer.

TaqMan Gene Expression Assays were used to measure messenger RNA (mRNA) abundance of VNN2, with *SDHA* as control gene. TaqMan Gene Expression Master Mix (cat. no. 4369016; Applied Biosystems, Foster City, CA), Assay-On-Demand (TaqMan Gene Expression Assays, Hs01546812_m1 VNN1, Hs00190581_m1 VNN2, Hs00417200_m1 SDHA; Applied Biosystems), and water were mixed (5:3:2), and complementary DNA (1:3 dilution) was added. The same was done using a SYBR Green assay for *VNN2* and *SDHA* as control gene (QuantiTect SYBR Green PCR Kit, Power SYBR Green PCR Master Mix, cat. no. 4367659, Applied Biosystems; Quantitect Primer Assay, Hs_VNN2_1_SG, cat. no. QT00034902 and Hs_SDHA_1_SG, cat. no. QT00059486, Qiagen).

A 7900HT Fast Real-Time PCR System (Applied Biosystems) was used for both methods. We used the following cycles: 2 minutes 50°C, 10 minutes 95°C, 50× (10 seconds 95°C/1 minute 60°C). Analysis was performed with SDS 2.2 software using the $2^{-\Delta CT}$ value.

Statistics

VNN2 threshold was defined based on SYBR Green PCR values, which divided a group of 770 patients from the ALL-BFM 2000 study into a training set (one third of the patients) and a test set (two thirds of the patients). The VNN2 threshold associated with a higher risk for relapse was defined based on the lowest *P* value in a univariate Cox model in the training set. This threshold was used for dichotomizing the patients in the test set. Samples with $2^{-\Delta\Delta CT} > 1.13$ (cutoff VNN2 transcript level) were tested by flow cytometry (FCM) based on sample availability. Event-free survival was defined

Table 2. Proteins identified in MRD VHR ALL by CSC

	SR											VHR							
	01	02	03	04	05	06	07	14	15	16	17	08	09	10	11	12	13	18	19
Adhesion and migration																			
VNN2												+	+		+	+			
VNN1		+		+							+	+	+		+	+			+
ITGAM											+	+	+		+		+		+
CD33			+										+	+	+		+		
CD302												+	+	+		+			+
CEAM1												+			+	+	+		
Signaling																			
TNR1B			+									+	+	+	+				
IGF1R								+	+		+	+	+	+	+	+	+	+	+
Immune response																			
CR1		+										+	+		+		+		
CR2		+								+		+	+	+	+		+		
Others																			
SORL									+			+	+	+	+				
2B19								+		+		+	+		+	+	+		
GI24		+	+			+						+		+	+	+	+		+

+, detected by CSC as described in Mirkowska et al.[12]

as the time from diagnosis to the date of last follow-up or first event. Events were nonresponse, relapse, secondary neoplasm, or death from any cause. Failure to achieve remission due to death before complete remission or nonresponse was considered as event at time 0. The Kaplan-Meier method was used to estimate survival rates; differences between groups were compared with the log-rank test. Cumulative incidence functions for competing events were constructed using the method of Kalbfleisch and Prentice and were compared with Gray's test.[24] Statistical analysis was done using GraphPad Prism version 8.0 (GraphPad Software). The prognostic value of VNN2 was analyzed with a Cox regression model including covariates that are known to be risk factors in the ALL-BFM 2000 study and used as covariates in another study[8]: ETV6-RUNX1 positivity, poor prednisone response, white blood cell count $\geq 100 \times 10^3/\mu L$, MRD low risk, MRD HR, and MRD slow early response. Statistical analysis was done using GraphPad Prism 8 (GraphPad software) and SAS 9.4 (SAS Institute, Cary, NC).

Results

A set of proteins implicated in cell adhesion and immune response is preferentially present on the surface of MRD$^+$ leukemia

To identify cell surface markers that are characteristic of resistant disease, we interrogated the cell surface proteomes of 19 B-cell precursor (BCP) ALL PDXs previously acquired using CSC technology.[12] This dataset included specimens from 8 patients with VHR ALL, as defined by persistence of MRD ($>5 \times 10^{-4}$) after induction chemotherapy, consolidation therapy, and 3 highly intensive postconsolidation blocks according to the ALL-BFM 2000 protocol,[21,25,26] and 11 patients with an excellent clinical outcome (SR ALL). We identified 13 proteins that were detected more frequently in VHR ALL (Table 2), including several surface proteins that are involved in cell adhesion and migration: the GPI-anchored vanin family of proteins (VNN1 and VNN2 [GPI-80]), with VNN2 being exclusively detected on the cell surface of VHR ALL cases, the immunoglobulin-like CEA family member CEAM1, the C-type lectin receptor CD302, and the sialic acid binding immunoglobulin-like lectin CD33, as well as ITGAM (CD11b), which is a subunit of the complement receptor 3 and has been linked to chemotherapy resistance in ALL.[27] Furthermore, the receptors for activated complement CR1 and CR2, as well as components of prosurvival signaling pathways (TNFR1B, IGF1R), were detected in VHR ALL cases.

The GPI-anchored surface protein VNN2 is associated with MRD and a higher risk for relapse

Given that VNN2 is implicated in early immature compartments and that we identified 2 members of the same vanin protein family in our experiment, we next focused on the validation of VNN2 in ALL. To explore retrospective banked samples, we first established a correlation between VNN2 RNA and protein expression in 34 PDXs derived from HR, MR, and SR patients based on their MRD after induction chemotherapy (Figure 1A). Detection of VNN2 by FCM correlated with detection of VNN2 mRNA by quantitative PCR (q-PCR) (Figure 1A). VNN2 was detected preferentially on the surface of leukemia cells from patients with MR ALL and HR ALL. We compared VNN2 expression by FCM on matched samples from 11 patients from diagnosis, relapse, and PDX to verify that VNN2 expression is maintained during disease evolution and in PDXs (supplemental Table 2). Thus PDXs constitute an acceptable model to study this phenotype. We then performed a retrospective quantitative RT-PCR analysis on banked RNA from 770 pediatric ALL

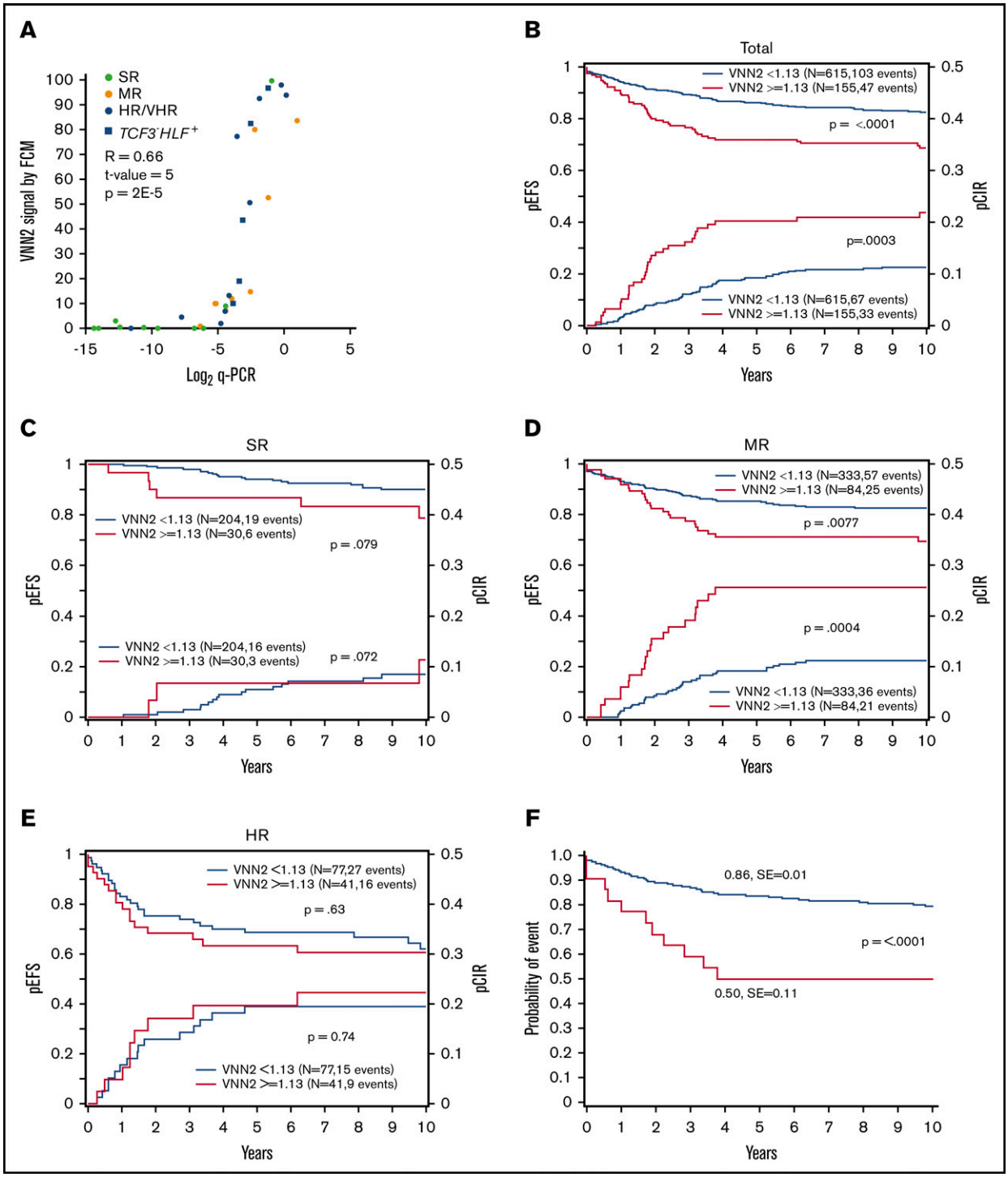

Figure 1. VNN2 expression is associated with an increased risk for relapse in BCP ALL. (A) VNN2 mRNA expression by q-PCR correlates with detection of VNN2 at the cell surface by FCM. PDXs from patients included in the ALL-BFM-2000 study were used for correlation. The percentage of $VNN2^+$ cells by FCM with respect to the fluorescence-minus-one control is plotted on the y-axis against the mRNA levels by q-PCR as logarithmic value of $2^{-\Delta CT}$ ($\Delta CT = CT_{VNN2} - CT_{SDHA}$) on the x-axis. MRD-based risk stratification in ALL-BFM-2000 is indicated as SR, eMR, and HR. Patients with the translocation t(17;19) leading to *TCF3-HLF* are highlighted as *TCF3-HLF*$^+$. (B) Five-year pEFS (upper part of the panel) and probability of cumulative incidence of relapse (pCIR; lower part of the panel) of 476 patients (test set) treated on the ALL-BFM 2000 study stratified according to VNN2 positivity by q-PCR. The cutoff for positivity was set to 1.13 ΔCT, as described in Materials and methods. (C-E) Five-year pEFS (upper part of the panel) and pCIR (lower part of the panel) of the same 476 patients in a subgroup analysis based on their risk stratification [SR (C), MR (D), and HR (E) for relapse] in the ALL-BFM-2000 study. A statistically significant difference was observed for pEFS and pCIR in $VNN2^+$ vs $VNN2^-$ patients in the MR group ($P < .01$). (F) Retrospective analysis of VNN2 expression by FCM on available archived samples from $VNN2^+$ ALL patients based on q-PCR. Sample selection is described in supplemental Figure 1. Twenty-two of 40 positive samples by q-PCR were confirmed $VNN2^+$ by FCM. Cutoff for VNN2 positivity by FCM > 10% (Materials and methods). pEFS of 22 $VNN2^+$ patients based on FCM is plotted in comparison with pEFS of 615 $VNN2^-$ patients based on q-PCR from the total retrospective cohort. $P < .0001$, log-rank test.

patients treated on the ALL-BFM-2000 protocol (Table 1). Using 294 (38%) of 770 patients as a training set, we established a cutoff (q-PCR value ≥1.13) to determine the association between risk and VNN2$^+$ samples (see Materials and methods) and explored the correlation between VNN2 positivity and outcome in a test set of the remaining 476 patients with BCP ALL (Figure 1B-E; supplemental Figure 1A). In total, 155 of 770 patients had VNN2 expression ≥ 1.13. The 5-year probability of event-free survival (pEFS) was inferior in VNN2$^+$ patients (0.87; standard error, 0.02 for VNN2 <1.13 and 0.67; standard error, 0.05 for VNN2 ≥1.13; $P <$ .0001) (Figure 1B). We detected a significant increase in relapses, predominantly in the MR ALL subgroup ($P = .0003$) (Figure 1D). In the HR group, the increased incidence of relapse for VNN2$^+$ patients was not significant, which may be explained by the comparable state of drug resistance in other subtypes of the HR cohort or the fact that some VNN2$^+$ patients may benefit from HR treatment intensification, including stem cell transplantation (Figure 1E). Thus, further exploration of this phenotype may be most relevant for the MR group, for which new markers to improve risk stratification are warranted. Importantly, using a Cox regression analysis, VNN2 was found to be an independent prognostic factor compared with MRD and other clinical factors (Table 3). We also noticed a higher proportion of central nervous system (CNS) involvement in VNN2$^+$ patients (6.4% in the retrospective cohort, 16% in the prospective cohort) compared with the frequency of CNS$^+$ patients in the ALL-BFM-2000 cohort (3.4% CNS$^+$; Tables 2 and 3).

For these retrospective analyses, biobanked material with bone marrow (BM) involvement >80% was selected. Because VNN2 is expressed in the normal myeloid compartment, residual myeloid cells may express higher levels of VNN2 and, thus, generate a background signal in the entire cohort. Given the strong correlation between RNA and FCM data, we propose to use FCM to determine VNN2 expression at the single-cell level in prospective studies. To gather pilot information, we used 40 of 155 VNN2$^+$ samples for which viably frozen specimens were available from the biobanks and confirmed VNN2 by FCM in 22 of 40 (supplemental Figure 1); this indicates that FCM may define VNN2 positivity more precisely. Eleven (50%) of these 22 VNN2$^+$ patients eventually relapsed, which again indicates that VNN2 expression is an indicator for resistant disease (Figure 1F). Taken together, pediatric BCP ALL leukemias with VNN2 expression are associated with a lower event-free survival and a higher MRD-based risk for relapse.

Table 3. Prognostic significance of VNN2 expression in a multivariable setting (n = 476)

Group	HR	LL	UL	P (χ^2)
Cox EFS				
MRD HR	5.16	2.58	10.32	<.001
VNN2	2.14	1.28	3.55	.003
SET	2.67	1.19	6.00	.017
WBC ≥100 000	2.01	1.08	3.73	.027
MRD SR	0.74	0.43	1.27	.275
Pred. resp.	0.71	0.33	1.52	.379
ETV6-RUNX1	0.93	0.51	1.70	.812
Cox RFS				
VNN2	1.97	1.13	3.44	.016
MRD HR	2.85	1.20	6.80	.018
WBC ≥100 000	2.17	1.12	4.21	.021
SER	2.41	1.01	5.74	.046
MRD SR	0.67	0.37	1.21	.182
ETV6-RUNX1	0.74	0.38	1.45	.379
Pred. resp.	0.81	0.35	1.86	.623

Analysis was performed on 476 samples from the test set from ALL-BFM 2000.
EFS, event-free survival; HR, hazard ratio; LL, lower limit of 95% confidence interval; Pred. resp, prednisone good responders; RFS, relapse-free survival; SER, slow early responders, a HR criterium; UL, upper limit of 95% confidence interval; WBC, white blood cell.

VNN2 is detected predominantly in MRD HR and MR patients by prospective FCM

To validate VNN2 in pediatric BCP ALL prospectively, we included VNN2 in the diagnostic FCM panel of the AIEOP-BFM ALL 2009 study. Positivity was defined as ≥10% of cells being positive compared with the internal cross-lineage, CD45^{bright} control (supplemental Figure 2). In total, 1069 patients were evaluated, of whom 103 were VNN2$^+$, which translates to 10% VNN2 positivity in BCP ALL (Figure 2A). We confirmed that VNN2 is detected predominantly in MRD HR and MR ALL patients and at lower frequency in MRD SR ALL (17%) compared with what has been reported[28] (Table 1). VNN2 is detected across different genetic subtypes (Figure 2B). It was associated with detection of CD11a, an integrin implicated in cell adhesion, but not with bilineage acute leukemia or mixed phenotype acute leukemia status (Figure 2B; supplemental Table 3). Of note, we detected VNN2 in all leukemias bearing the translocation t(17;19)(q22;p13) (Figure 1A), which results in the oncogenic *TCF3-HLF* transcription factor fusion and defines a rare, but generally incurable, ALL subtype (<1% of pediatric ALL).[29,30] Having established an international consortium to study the genomic landscape of this rare subtype,[5] we evaluated 18 *TCF3-HLF*$^+$ ALL samples by FCM and confirmed consistent positivity for VNN2 in patient samples and in PDXs (Figures 1A, 2C). VNN2 positivity remained stable when comparing samples taken at diagnosis and at day 15 from 9 patients with ALL (Figure 2D). Matched samples from diagnosis and first relapse were available for 22 cases, selected from a cohort of isolated and combined BM (involvement of extramedullary compartment, ALL-REZ BFM 2002 study) based on sample availability. Two samples were VNN2$^+$ at both diagnosis and relapse, whereas 5 cases were positive at first relapse (Figure 2E). Relapses in VNN2$^+$ patients occurred very early/early compared with VNN2$^-$ patients (86% vs 26.6%; $P = .02$). Taking advantage of our ex vivo drug response profiling platform,[31] we screened 10 VNN2$^+$ ALL samples for sensitivity to standard chemotherapeutic agents of induction therapy. Comparison with 8 samples from ALL samples from the SR group revealed lower sensitivity of VNN2 ALL to dexamethasone, bortezomib, and anthracyclines (Figure 2E), further supporting the notion that VNN2$^+$ ALL is associated with chemoresistance.

Because VNN2 defines a human FLHSC compartment[18] and marks human cord blood–derived primitive CD34$^-$ HSCs,[19] we evaluated BM and PB samples from healthy adults and children. VNN2 was readily detectable in HSCs from normal BM, including HSC subpopulations with very high VNN2 surface expression (supplemental Figure 3). Intriguingly, VNN2 was not expressed in mobilized PB HSCs. As expected, VNN2 was highly expressed on mature granulocytes and monocytes and weakly expressed on other lymphocytes.

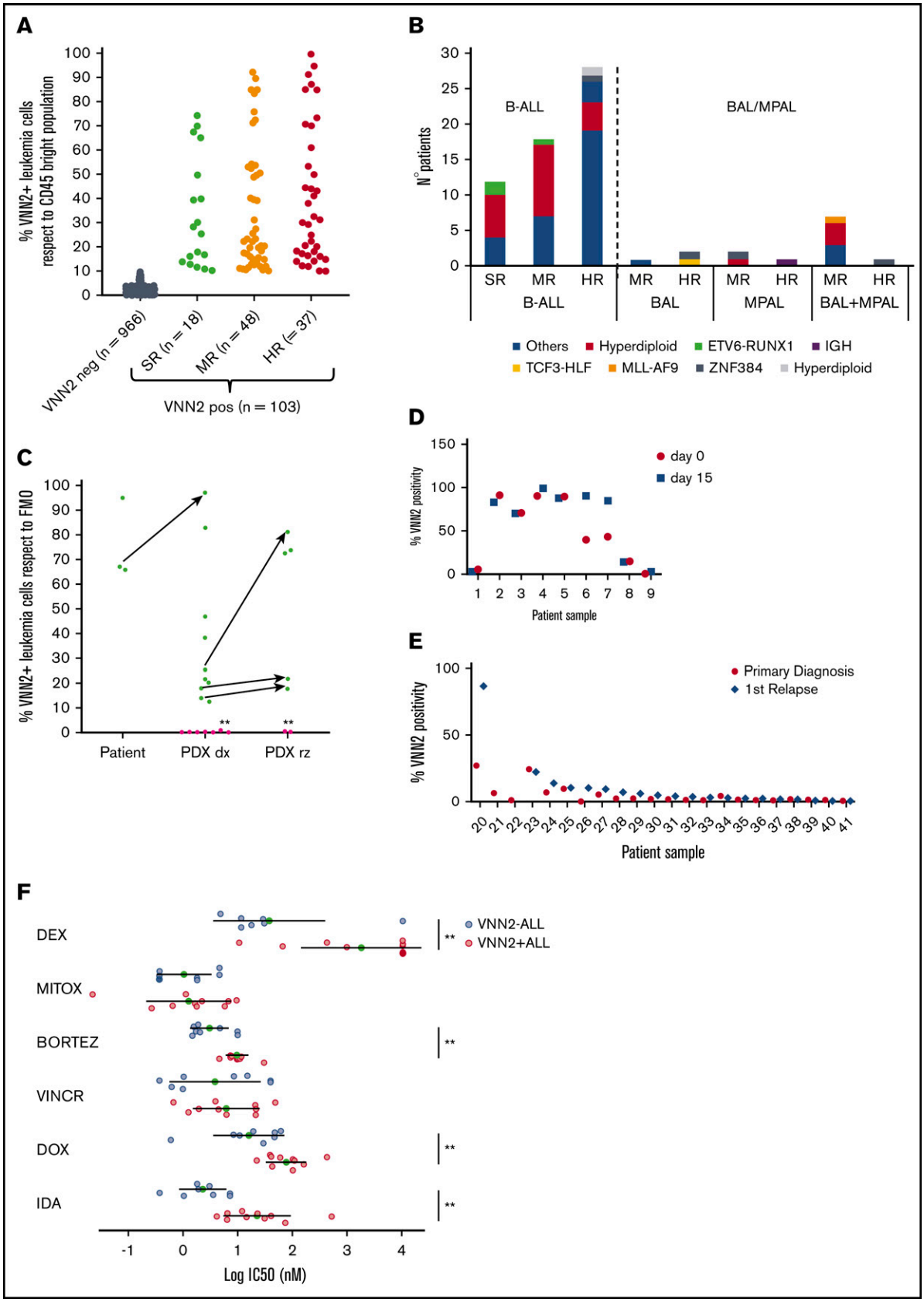

Figure 2. Prospective validation of VNN2 by FCM confirms its association with MRD. (A) FCM evaluation of VNN2 in diagnostic samples from 1069 B-cell ALL patients enrolled in the AIEOP-BFM 2009 study. (B) Classification of 72 BFM 2009 VNN2^{+} patients based on cytogenetic information and FCM data. Cytogenetic data

These results support the use of FCM for VNN2 detection in clinical studies. The prognostic value of VNN2 will require further maturation of the clinical data.

The gene expression signature of VNN2$^+$ ALL reveals immune and cell adhesion features, as well as myeloid characteristics

To obtain a gene expression signature associated with VNN2 expression, we performed a transcriptome analysis of 50 B-cell ALL (B-ALL) leukemia samples with low to high VNN2 RNA expression with *TCF3-HLF*–rearranged, *TCF3-PBX1*–rearranged, IKZF1^{plus}, IKZF1^{deleted}, hyperdiploid, hypodiploid, and additional ALL without known genetic features (so-called B-others) (Figure 3A). After fitting a linear model using VNN2 as a predictor of gene expression, we identified a VNN2 signature with 1061 genes that strongly correlated with VNN2; 549 and 512 genes were positively and negatively correlated, respectively. This VNN2 signature includes some of the surface proteins that we detected in HR MRD ALL by proteomics (Figure 3A). We found an overrepresentation of features functionally related to cell adhesion, the immune response, and the JAK-STAT pathway (Figure 3B). By gene-set enrichment analysis (Figure 3C) and using a different method based on text mining annotations (Figure 3D; supplemental Table 4), we found an association between the VNN2 signature and myeloid features and detected a significant reduction in PAX5 expression, which is in line with the genomic features of VNN2$^+$ *TCF3-HLF* ALL.[5] However, VNN2 appears to be dispensable for leukemia maintenance and propagation, because we could generate and serially passage 2 *VNN2*-knockout samples using clustered regularly interspaced short palindromic repeats/Cas9 in NSG mice (supplemental Figure 1D). More studies will be required to carefully evaluate the impact of VNN2 on sites of leukemia involvement in this PDX model.

VNN2$^+$ ALL includes different B-ALL subtypes, combining inactivation of B-cell developmental genes, frequent homozygous *CDKN2A/B* deletions, and mutations affecting epigenetic regulators

To identify underlying genetic alterations, we applied next-generation sequencing analysis integrating short and large insert size paired-end whole-genome and whole-exome sequencing to a discovery cohort consisting of 22 VNN2$^+$, *TCF3-HLF*$^-$ diagnostic samples (supplemental Figure 4). Genomic information from *TCF3-HLF*$^+$ patients was available from our previous study.[5]

Of note, we detected frequent monoallelic deletions of *PAX5*, almost always combined with deletion of *CDKN2A/B* and sometimes combined with deletions of *IKZF1* (Figure 4). In 1 sample we detected the PAX5 P80R mutation, in combination with biallelic deletion of *CDKNA/B*. We observed mutations affecting *IKZF1* in 8 of 22 samples (36%), primarily hemizygous deletions (5/8), but also homozygous deletions (2/8) and 1 single-nucleotide variant. Five of the patients (23%) with *IKZF1* deletions, all from non-SR subgroups, fit the definition of IKZF1^{plus} cases, which represent a new subtype with very poor outcome on the AIEOP-BFM protocol.[8] This frequency of *IKZF1* deletions is expected in ALL,[32] but IKZF1-^{plus} appears to be enriched compared with the 6% frequency reported previously.[8] In addition to *TCF3-HLF* fusions, we identified rearrangements of *TCF3* with *ZNF384*, a recurrent mutation in ALL,[33] as well as with *JAK2*, which has not been described previously. We also found a *JAK2-BCR* fusion, previously described in *BCR-ABL*–like ALL.[34] Thus, the VNN2 phenotype was detected across different leukemia-initiating lesions, including IKZF1^{plus}, possibly B-ALLs corresponding to the recently defined PAX5alt subtype,[1] *TCF3*-rearranged ALL, and, rarely, *BCR-ABL*–like subtypes.

As expected in these B-ALL subtypes, we detected frequent gain-of-function single-nucleotide variants in the Ras pathway, such as *PTPN11*, *NRAS*, and *KRAS* (Figure 4; supplemental Table 6). In addition, we noticed frequent mutations in epigenetic regulators in 13 of 22 (60%) VNN2$^+$ patients at first diagnosis (Figure 4), suggesting a marked increase compared with frequencies reported previously for pediatric B-ALL (12/42 = 30%).[35] Interestingly, we did not find these epigenetic mutations in *TCF3-HLF* cases.[5] To confirm possible enrichment of epigenetic mutations in MRD MR ALL, we performed targeted sequencing of the histone-lysine methyltransferases *EZH2*, *KMT2D*, and *SETD2*, as well as the lysine demethylase *KDM6A*, on 185 samples from the retrospective ALL-BFM-2000 MRD-MR cohort in which we also determined VNN2 mRNA levels by q-PCR (supplemental Table 7). In this MRD MR cohort, 15 of 35 (43%) VNN2$^+$ patients and 19 of 150 (13%) VNN2$^-$ patients displayed ≥1 mutation in these 4 genes. Mutations in this functional class have been reported for a subset of patients with PAX5alt and PAX5 P80R.[1] Taken together, we identify a VNN2 signature that is clearly associated with resistance to chemotherapy but that is found in different molecular B-ALL subtypes, mostly with lesions in B-cell developmental genes and, frequently, in genes affecting epigenetic modification. These features should be included in upcoming prospective international trials to evaluate their contribution to more precise risk stratification in ALL.

Discussion

This study identifies a recurrent VNN2 signature that is associated with increased resistance to chemotherapy in 10% of BCP ALL cases across different ALL subtypes, primarily stratified in the MR and HR groups based on resistance to treatment, as assessed by

Figure 2. (continued) were available for 72 of 103 patients identified by FCM. (C) VNN2 expression by FCM identifies *TCF3-HLF*–rearranged samples. Green dots indicate *TCF3-HLF*–rearranged samples (patient and PDX), and pink dots indicate *TCF3-PBX1*–rearranged PDX samples. Arrows indicate matched patient-PDX sample or matched xenograft samples at diagnosis-relapse. Asterisks (*) indicate matched diagnosis-relapsed samples. *TCF3-HLF* rearranged samples scored positive for VNN2 by FCM (>10%). (D) Analysis of VNN2 in matched samples from 9 patients taken at diagnosis of ALL (day 0) and at day 15 by FCM. (E) Comparison of matched diagnosis (black circles) and relapse (gray rhombus) pairs indicated conservation of VNN2 positivity; in some cases, an increase in VNN2 from diagnosis to relapse could be observed. FCM was used to evaluate VNN2 of matched diagnosis and first relapse of 22 patients with ALL. (F) Ex vivo drug response profiling of 10 VNN2$^+$ ALL samples (red circles) compared with 8 VNN2$^-$ SR cases (blue circles). Patient samples were tested for dexamethasone (DEX), mitoxantrone (MITOX), bortezomib (BORTEZ), vincristine (VINCR), doxorubicin (DOX), and idarubicin (IDA). $^{**}P < .05$. BAL, biphenotypic acute leukemia according to EGIL classification; B-ALL, B-cell ALL; dx, diagnosis; FMO, fluorescence-minus-one; IC50, 50% inhibitory concentration; MPAL, mixed phenotype ALL, according to World Health Organization classification[23]; rz, relapse; SE, standard error.

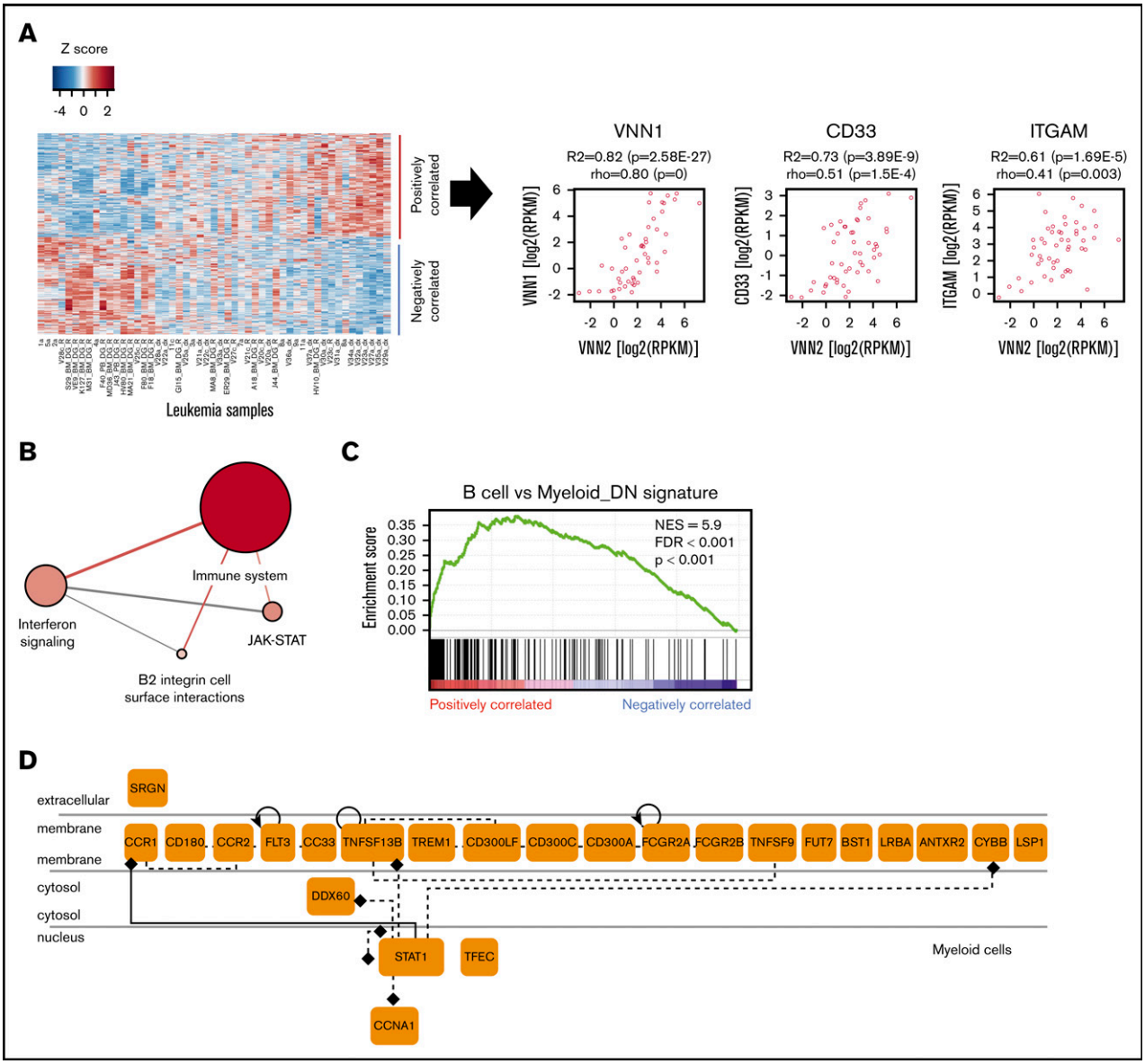

Figure 3. The signature of VNN2^{+} ALL is enriched with myeloid features and functional annotations related to immune response, interferon signaling, cell adhesion, and the JAK-STAT pathway. (A) Heat map with 1061 differentially expressed genes showing the transcriptome signature of 50 B-ALL samples ordered by increasing VNN2 RNA expression (left panel). Using edgeR,[48] a linear model was fitted across the dataset of 50 ALL samples using VNN2 expression as predictor of gene expression. Genes that showed a significant linear relationship with VNN2 expression were selected (false discovery rate [FDR] ≤0.01). Genes were additionally filtered using Spearman correlation (FDR ≤0.04). A total of 549 genes and 512 genes appeared to be positively or negatively correlated with VNN2, respectively. Genes positively correlated with VNN2 include 3 genes that were identified by proteomics in an independent cohort using CSC technology (right panels). (B) Positively correlated genes were grouped by pathways using the online tool and database ConsensusPathDB[49] (FDR ≤0.01). The most significantly overrepresented pathways (according to *P* value) included the immune system, interferon signaling, β-2 integrin–mediated interactions, and the JAK-STAT signaling pathway. Node size indicates the number of genes contained and the color refers to significance (*P* value). Two nodes are connected by a line if they share members. The line width reflects the relative overlap between the nodes, whereas the line color represents the number of shared members that are also found in the input. (C) Enrichment plot for the myeloid signature obtained after performing gene set enrichment analysis.[50] (D) Components of the VNN2^{+} ALL signature generated using the Genomatix genome analyzer reveal functional annotations related to myeloid cells and their cellular location (adjusted $P \leq .05$; $P \leq .01$). Lines between genes indicate a functional association. The line type indicates the evidence level. Dashed lines indicate a functional association based on cocitation or experimental validation. Solid lines indicate a functional association based on expert curation. Diamonds indicate that a gene carries a binding site of the associated transcription factor. Arrows indicate that a gene is altered by the associated gene. Curved lines indicate that a gene alters itself on a transcriptional or protein level. The line type indicates the evidence level. Myeloid_DN, myeloid gene expression signature; NES, normalized enrichment score.

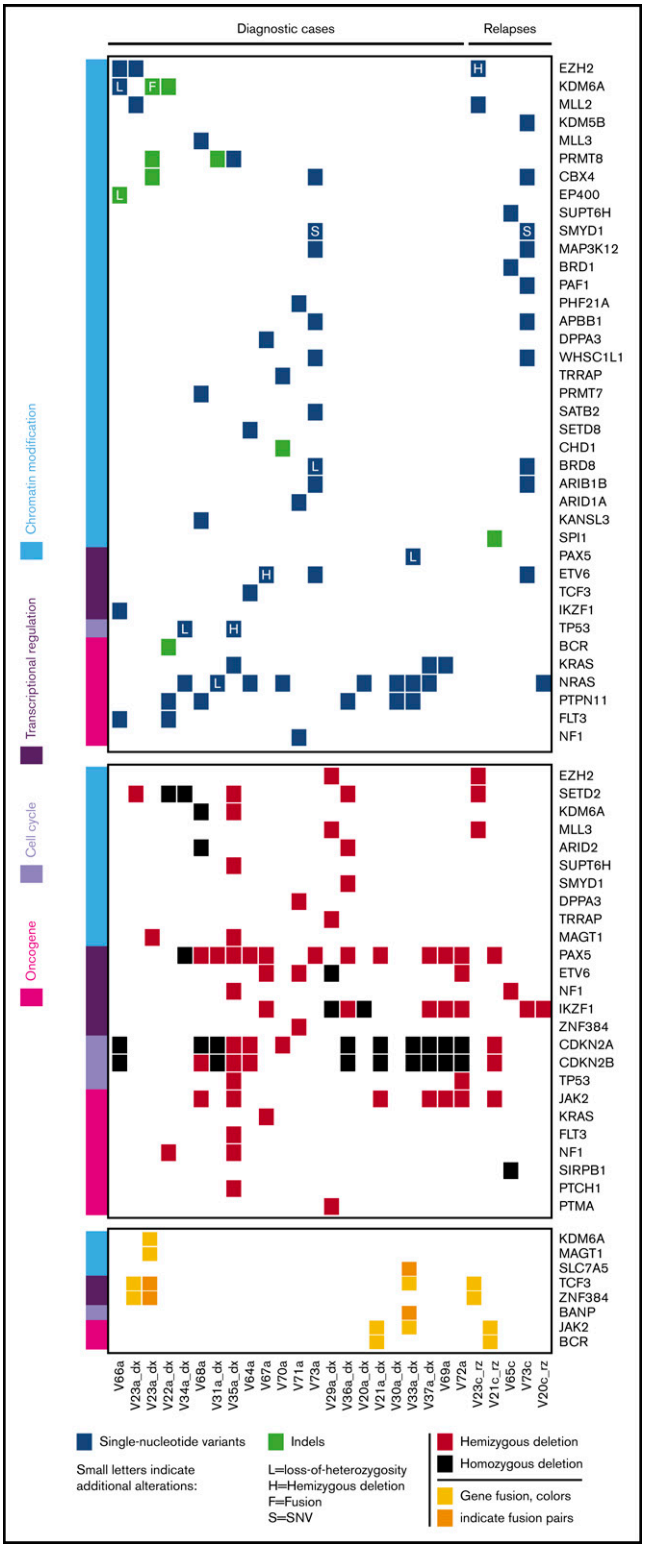

Figure 4. Whole-exome and transcriptome sequencing identified frequent deletions in *PAX5*, *IKZF1*, *CDKN2A/B* and mutations in epigenetic regulators in VNN2$^+$ patients. Whole-exome sequencing was performed in 27 VNN2$^+$ patient samples (22 diagnosis, 5 relapse), and transcriptome sequencing was performed in 16 VNN2$^+$ patient samples (13 diagnosis, 3 relapse). Details about sample selection are described in supplemental Figure 4. Sample identifiers

MRD. Most of the relapses in ALL still occur in the MR group by MRD.[8,36,37] Although patients with more resistant leukemia may need a different intervention, many patients in the MR group may benefit instead from a reduction in treatment intensity to minimize long-term toxicity.

Expression and cell surface display of the glycosylphosphatidylinositol-anchored surface protein VNN2/GPI-80 is associated with myeloid features that are not captured by current definitions of bilineage and mixed immunophenotypes by diagnostic FCM.[23] VNN2 itself was recently identified as a marker of self-renewing human FLHSCs[18] and cord blood–derived HSCs.[19] In this study, we detected strong VNN2 expression in subsets of human adult BM HSCs from healthy individuals, confirming its implication in the very early stages of hematopoiesis. We also found recurrent surface markers associated with VNN2, including VNN1 and members of the integrin and selectin family. Functionally, these proteins are involved in cell adhesion and processes linked to inflammation. VNN2 has been implicated in inflammation, contributing to leukocyte adhesion and migration to inflammatory sites in association with cell surface integrins.[17] It is conceivable that this signature reflects functional states that are important for interactions with the leukemia microenvironment and involvement at sanctuary sites. Given the strong correlation between mRNA and protein levels, VNN2 is regulated at the transcriptional level. Because of the marked expression of VNN2 in the normal myeloid compartment, FCM represents the methodology of choice to detect VNN2 positivity at the single-cell level on ALL cells.

From a genomics standpoint, we detected a reduction in *PAX5* gene dosage in the majority of samples that we tested thus far, which is reminiscent of our observation in *TCF3-HLF*$^+$ ALL.[5] In our cohort, events leading to *PAX5* loss of function were primarily monoallelic, which is in contrast with the majority of the samples for 2 recently described entities in ALL, PAX5alt[1] and PAX5 P80R,[38] in which both alleles of *PAX5* are generally affected. Indeed, VNN2 expression was also detected in the IKZF1^{plus} ALL subtype, which has been identified based on the combination of *IKZF1* deletions that co-occurred with deletions in *CDKN2A*, *CDKN2B*, *PAX5*, or *PAR1* in the absence of *ERG* deletions, marking a subtype with poor outcomes in patients with MRD MR ALL or MRD HR ALL.[8]

Of note, we detected genetic alterations affecting epigenetic modifiers in 13 of 22 VNN2$^+$ ALLs. The methyltransferases *EZH2*, *KMT2D*, and *SETD2*, as well as the lysine demethylase *KDM6A*, were affected recurrently. Similar mutations have been reported in a subset of PAX5alt and PAX5 P80R B-ALL patients.[1] Loss-of-function mutations in *EZH2* have been reported in T-cell ALL and B-ALL at low frequencies,[39-41] as well as in myeloid disorders.[42] Moreover, loss-of-function mutations in *EZH2* have very recently been associated with poor outcome in AML.[43] *MLL2* deficiency impedes B-cell differentiation and is a driver of lymphoma in vivo.[44] Moreover, mutations in *SETD2* and *KDM6A* have been reported to be enriched in relapsed pediatric B-ALL,[45] which suggests that they could be relevant for chemotherapy resistance. Inactivation of *KDM6A* is crucial in B-cell lymphoma[44] and T-cell ALL,[46] contributing to tumorigenesis

Figure 4. (continued) are shown at the bottom of the figure. «V_a» indicates samples at diagnosis, and «V_c» indicates samples at relapse. Samples in which transcriptome sequencing was performed can be identified by an additional «_dx» or «_rz» at the end of the identifier. dx, diagnosis; rz, relapse.

by deregulation of complexes that control histone methylation in important regulatory regions.[47]

Taken together, we have identified a new signature in ALL, whereby surface expression of VNN2 is associated with increased resistance to induction chemotherapy. Our results support a prospective evaluation of VNN2 by FCM in the ongoing AIEOP-BFM ALL trial. We propose to explore the prognostic significance of this marker, along with more complex genomic information, to improve the identification of patients who will eventually relapse, in particular those with IR ALL, the largest risk group, on the current treatment protocol.

Acknowledgments

The authors thank Renate Siegenthaler for data management, Astrid Mecklenbräuker for assistance with FCM, and Yi-Chien Tsai and Silvia Jenni for technical help.

This work was supported by Kinderkrebsforschung Schweiz (J.-P.B.), Krebsliga Zurich (J.-P.B.), the Swiss National Science Foundation (310030-156407 and 310030-182269) (J.-P.B.), the Sassella Foundation (J.-P.B.), the Hanne Liebermann Foundation (J.-P.B.), Clinical Research Priority Program (CRPP) Human Hemato-Lymphatic Diseases (HHLD) (J.-P.B.), and Czech Ministry of Health NV18-03-00343 (E.M.).

Authorship

Contribution: V.R.M., M. Schütte, A.R., G.C., T.R., H.-J.W., N.S., P.M., A.H., M.T., C.M., A.S., M.R., E.M., B. Bornhauser, B. Buldini, P.S., O.M., E.V., B.M., M.J.B., T.L.S., M.Z., and B.W. performed experiments and analyzed data; Q.A.N. analyzed data; M.D., A.A., M.B., G.B., G.G., G.t.K., R.P.-G., M.H.-H., F.N., C.E., M. Schrappe, and M. Stanulla provided samples and clinical data; B. Bornhauser and J.-P.B. wrote the manuscript; and B. Bornhauser, M.-L.Y., and J.-P.B. conceived and supervised the study.

Conflict of interest disclosure: M. Schütte is an employee of Alacris Theranostics GmbH. The remaining authors declare no competing financial interests.

ORCID profiles: T.R., 0000-0002-7998-1651; Hans-J.W., 0000-0002-0327-9209; M.B., 0000-0001-5514-5010; G.teK., 0000-0001-7143-4795; E.V., 0000-0002-9705-7083; M.J.B., 0000-0003-1581-2020; C.E., 0000-0003-1039-2872; B.W., 0000-0002-3923-1610; J-P.B., 0000-0001-6571-6227.

Correspondence: Jean-Pierre Bourquin, Department of Oncology, University Children's Hospital Zurich and Children's Research Center, Steinwiesstr 75, 8032 Zurich, Switzerland; e-mail: jean-pierre.bourquin@kispi.uzh.ch.

References

1. Gu Z, Churchman ML, Roberts KG, et al. PAX5-driven subtypes of B-progenitor acute lymphoblastic leukemia. *Nat Genet*. 2019;51(2):296-307.
2. Flohr T, Schrauder A, Cazzaniga G, et al; International BFM Study Group (I-BFM-SG). Minimal residual disease-directed risk stratification using real-time quantitative PCR analysis of immunoglobulin and T-cell receptor gene rearrangements in the international multicenter trial AIEOP-BFM ALL 2000 for childhood acute lymphoblastic leukemia. *Leukemia*. 2008;22(4):771-782.
3. Moorman AV, Enshaei A, Schwab C, et al. A novel integrated cytogenetic and genomic classification refines risk stratification in pediatric acute lymphoblastic leukemia. *Blood*. 2014;124(9):1434-1444.
4. O'Connor D, Enshaei A, Bartram J, et al. Genotype-Specific minimal residual disease interpretation improves stratification in pediatric acute lymphoblastic leukemia. *J Clin Oncol*. 2018;36(1):34-43.
5. Fischer U, Forster M, Rinaldi A, et al. Genomics and drug profiling of fatal TCF3-HLF-positive acute lymphoblastic leukemia identifies recurrent mutation patterns and therapeutic options. *Nat Genet*. 2015;47(9):1020-1029.
6. Holmfeldt L, Wei L, Diaz-Flores E, et al. The genomic landscape of hypodiploid acute lymphoblastic leukemia. *Nat Genet*. 2013;45(3):242-252.
7. Mullighan CG, Goorha S, Radtke I, et al. Genome-wide analysis of genetic alterations in acute lymphoblastic leukaemia. *Nature*. 2007;446(7137):758-764.
8. Stanulla M, Dagdan E, Zaliova M, et al; International BFM Study Group. IKZF1^{plus} defines a new minimal residual disease-dependent very-poor prognostic profile in pediatric B-cell precursor acute lymphoblastic leukemia. *J Clin Oncol*. 2018;36(12):1240-1249.
9. Roberts KG, Li Y, Payne-Turner D, et al. Targetable kinase-activating lesions in Ph-like acute lymphoblastic leukemia. *N Engl J Med*. 2014;371(11):1005-1015.
10. Hussein SMI, Puri MC, Tonge PD, et al. Genome-wide characterization of the routes to pluripotency [published correction appears in *Nature*. 2015;523(7562):626]. *Nature*. 2014;516(7530):198-206.
11. Hofmann A, Gerrits B, Schmidt A, et al. Proteomic cell surface phenotyping of differentiating acute myeloid leukemia cells. *Blood*. 2010;116(13):e26-e34.
12. Mirkowska P, Hofmann A, Sedek L, et al. Leukemia surfaceome analysis reveals new disease-associated features. *Blood*. 2013;121(25):e149-e159.
13. Granjeaud S, Naquet P, Galland F. An ESTs description of the new vanin gene family conserved from fly to human. *Immunogenetics*. 1999;49(11-12):964-972.
14. Kaskow BJ, Proffitt JM, Blangero J, Moses EK, Abraham LJ. Diverse biological activities of the vascular non-inflammatory molecules - the vanin pantetheinases [published correction appears in *Biochem Biophys Res Commun*. 2012;422(4):786]. *Biochem Biophys Res Commun*. 2012;417(2):653-658.
15. Nitto T, Onodera K. Linkage between coenzyme a metabolism and inflammation: roles of pantetheinase. *J Pharmacol Sci*. 2013;123(1):1-8.

16. Aurrand-Lions M, Galland F, Bazin H, Zakharyev VM, Imhof BA, Naquet P. Vanin-1, a novel GPI-linked perivascular molecule involved in thymus homing. *Immunity*. 1996;5(5):391-405.

17. Yoshitake H, Takeda Y, Nitto T, Sendo F, Araki Y. GPI-80, a beta2 integrin associated glycosylphosphatidylinositol-anchored protein, concentrates on pseudopodia without association with beta2 integrin during neutrophil migration. *Immunobiology*. 2003;208(4):391-399.

18. Prashad SL, Calvanese V, Yao CY, et al. GPI-80 defines self-renewal ability in hematopoietic stem cells during human development. *Cell Stem Cell*. 2015;16(1):80-87.

19. Matsuoka Y, Sumide K, Kawamura H, Nakatsuka R, Fujioka T, Sonoda Y. GPI-80 expression highly purifies human cord blood-derived primitive CD34-negative hematopoietic stem cells. *Blood*. 2016;128(18):2258-2260.

20. Cario G, Zimmermann M, Romey R, et al. Presence of the P2RY8-CRLF2 rearrangement is associated with a poor prognosis in non-high-risk precursor B-cell acute lymphoblastic leukemia in children treated according to the ALL-BFM 2000 protocol. *Blood*. 2010;115(26):5393-5397.

21. Schrappe M. Minimal residual disease: optimal methods, timing, and clinical relevance for an individual patient. *Hematology Am Soc Hematol Educ Prog*. 2012;2012:137-142.

22. Attarbaschi A, Mann G, Panzer-Grümayer R, et al. Minimal residual disease values discriminate between low and high relapse risk in children with B-cell precursor acute lymphoblastic leukemia and an intrachromosomal amplification of chromosome 21: the Austrian and German acute lymphoblastic leukemia Berlin-Frankfurt-Munster (ALL-BFM) trials. *J Clin Oncol*. 2008;26(18):3046-3050.

23. Dworzak MN, Buldini B, Gaipa G, et al; International-BFM-FLOW-network. AIEOP-BFM consensus guidelines 2016 for flow cytometric immunophenotyping of pediatric acute lymphoblastic leukemia. *Cytometry B Clin Cytom*. 2018;94(1):82-93.

24. Kalbfleisch JD, Prentice RL. The Statistical Analysis of Failure Time Data. New York, NY: John Wiley & Sons, Inc.; 1980.

25. Schrappe M, Hunger SP, Pui CH, et al. Outcomes after induction failure in childhood acute lymphoblastic leukemia. *N Engl J Med*. 2012;366(15):1371-1381.

26. Eckert C, von Stackelberg A, Seeger K, et al. Minimal residual disease after induction is the strongest predictor of prognosis in intermediate risk relapsed acute lymphoblastic leukaemia - long-term results of trial ALL-REZ BFM P95/96. *Eur J Cancer*. 2013;49(6):1346-1355.

27. Rhein P, Mitlohner R, Basso G, et al. CD11b is a therapy resistance- and minimal residual disease-specific marker in precursor B-cell acute lymphoblastic leukemia. *Blood*. 2010;115(18):3763-3771.

28. Conter V, Bartram CR, Valsecchi MG, et al. Molecular response to treatment redefines all prognostic factors in children and adolescents with B-cell precursor acute lymphoblastic leukemia: results in 3184 patients of the AIEOP-BFM ALL 2000 study. *Blood*. 2010;115(16):3206-3214.

29. Hunger SP, Ohyashiki K, Toyama K, Cleary ML. Hlf, a novel hepatic bZIP protein, shows altered DNA-binding properties following fusion to E2A in t(17;19) acute lymphoblastic leukemia. *Genes Dev*. 1992;6(9):1608-1620.

30. Inukai T, Hirose K, Inaba T, et al. Hypercalcemia in childhood acute lymphoblastic leukemia: frequent implication of parathyroid hormone-related peptide and E2A-HLF from translocation 17;19. *Leukemia*. 2007;21(2):288-296.

31. Frismantas V, Dobay MP, Rinaldi A, et al. Ex vivo drug response profiling detects recurrent sensitivity patterns in drug-resistant acute lymphoblastic leukemia. *Blood*. 2017;129(11):e26-e37.

32. Mullighan CG, Su X, Zhang J, et al; Children's Oncology Group. Deletion of IKZF1 and prognosis in acute lymphoblastic leukemia. *N Engl J Med*. 2009;360(5):470-480.

33. Yasuda T, Tsuzuki S, Kawazu M, et al. Recurrent DUX4 fusions in B cell acute lymphoblastic leukemia of adolescents and young adults [published correction appears in *Nat Genet*. 2016;48(12):1591]. *Nat Genet*. 2016;48(5):569-574.

34. Roberts KG, Morin RD, Zhang J, et al. Genetic alterations activating kinase and cytokine receptor signaling in high-risk acute lymphoblastic leukemia. *Cancer Cell*. 2012;22(2):153-166.

35. Mar BG, Bullinger LB, McLean KM, et al. Mutations in epigenetic regulators including SETD2 are gained during relapse in paediatric acute lymphoblastic leukaemia. *Nat Commun*. 2014;5(1):3469.

36. Vora A, Goulden N, Wade R, et al. Treatment reduction for children and young adults with low-risk acute lymphoblastic leukaemia defined by minimal residual disease (UKALL 2003): a randomised controlled trial. *Lancet Oncol*. 2013;14(3):199-209.

37. Popov AM, Verzhbitskaya Ty, Fechina LG, Shestopalov AV, Plyasunova SA. Acute leukemias: immunophenotypic differences between blast cells and their nonneoplastic analogues in bone marrow. *Clin Oncohematol*. 2016;9(3):302-313.

38. Bastian L, Schroeder MP, Eckert C, et al. PAX5 biallelic genomic alterations define a novel subgroup of B-cell precursor acute lymphoblastic leukemia. *Leukemia*. 2019;33(8):1895-1909.

39. Ntziachristos P, Tsirigos A, Van Vlierberghe P, et al. Genetic inactivation of the polycomb repressive complex 2 in T cell acute lymphoblastic leukemia. *Nat Med*. 2012;18(2):298-301.

40. Schäfer V, Ernst J, Rinke J, et al. EZH2 mutations and promoter hypermethylation in childhood acute lymphoblastic leukemia. *J Cancer Res Clin Oncol*. 2016;142(7):1641-1650.

41. Chase A, Cross NC. Aberrations of EZH2 in cancer. *Clinical Cancer Res*. 2011;17(9):2613-2618.

42. Nikoloski G, Langemeijer SM, Kuiper RP, et al. Somatic mutations of the histone methyltransferase gene EZH2 in myelodysplastic syndromes. *Nat Genet*. 2010;42(8):665-667.

43. Saygin C, Hirsch C, Przychodzen B, et al. Mutations in DNMT3A, U2AF1, and EZH2 identify intermediate-risk acute myeloid leukemia patients with poor outcome after CR1. *Blood Cancer J*. 2018;8(1):4.

44. Ortega-Molina A, Boss IW, Canela A, et al. The histone lysine methyltransferase KMT2D sustains a gene expression program that represses B cell lymphoma development. *Nat Med*. 2015;21(10):1199-1208.

45. Mar BG, Kahn J, Zon RL, et al. SETD2 heterozygous loss in leukemia leads to chemotherapy resistance through attenuation of the DNA damage response. *Blood*. 2015;130(24):2631-2641.

46. Ntziachristos P, Tsirigos A, Welstead GG, et al. Contrasting roles of histone 3 lysine 27 demethylases in acute lymphoblastic leukaemia. *Nature*. 2014;514(7523):513-517.

47. Wang L, Shilatifard A. UTX mutations in human cancer. *Cancer Cell*. 2019;35(2):168-176.

48. Robinson MD, McCarthy DJ, Smyth GK. edgeR: a Bioconductor package for differential expression analysis of digital gene expression data. *Bioinformatics*. 2010;26(1):139-140.

49. Herwig R, Hardt C, Lienhard M, Kamburov A. Analyzing and interpreting genome data at the network level with ConsensusPathDB. *Nat Protoc*. 2016;11(10):1889-1907.

50. Subramanian A, Tamayo P, Mootha VK, et al. Gene set enrichment analysis: a knowledge-based approach for interpreting genome-wide expression profiles. *Proc Natl Acad Sci USA*. 2005;102(43):15545-15550.